Global NEST Journal, Vol 27, No X, pp 1-10

Investigation on the performance of single slope solar still with different absorber plates and condenser

Virumandampalayam Perumal Krishnamurthy[1*], Debabrata Barik[2*], Manivel Chinnappandi[3], K. Durga Syam Prasad[4], Subramaniam Prabagaran.[5] and Kandasamy Raju[6]

[1]Research Scholar, Department of Mechanical Engineering, Karpagam Academy of Higher Education, Coimbatore–641 021, India.

[2]Department of Mechanical Engineering and Centre for Energy and Environment, Karpagam Academy of Higher Education, Coimbatore–641021, India.

[3]Department of Mechanical Engineering, NPR College of Engineering and Technology, Natham, Dindigul, Tamil Nadu, India–624 401.

[4]Department of Electrical and Electronics Engineering, Vignan's Institute of Information Technology, Visakhapatnam, Andhara Pradesh, India.

[5]Karpagam Innovation and Incubation Council, Coimbatore, Tamilnadu, India - 641 021.

[6]Associate Professor Department of Mechanical Engineering, M. Kumarasamy College of Engineering, Karur, Tamil Nadu, Inida.

Received: 28/08/2024, Accepted: 05/06/2025, Available online: 16/06/2025

*to whom all correspondence should be addressed: e-mail: vpkkalai2010@gmail.com, debabrata93@gmail.com

https://doi.org/10.30955/gnj.06728

Graphical abstract

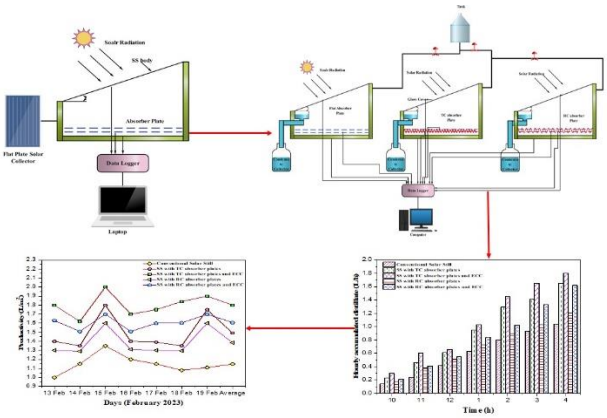

Abstract

Solar distillation is a low-maintenance and energy-saving way to turn salt water into potable water. The main problem with the desalination process is that the system's slow evaporation and condensation rate produces a low output rate of fresh water. An external copper condenser (ECC), two modified absorbing plates, and a single slope solar still (SS) are used to create a modified solar still (MSS) in this project. Evaporation rates may be increased by increasing the surface area of the absorber plates, which in turn enhances heat transfer to the basin water. The ECC is designed so that its cold surface area and the glass surface are more significant, increasing the condensation rate. This study compares the performance of the conventional solar still (CSS), the solar still with triangular channelled (TC) and ECC (SSTCE), the solar still with triangular channelled (TC) with no ECC (SSTC), and the solar still with rectangular channelled (RC) and no ECC (SSRC) over February to determine the most effective and efficient. The ECC-equipped SS model achieved the most excellent average productivity (1.8 ± 0.2 L/m^2) in the experimentation. The highest mean instantaneous efficiency with SS, SSTC, and SSTCE is 19.3 ± 2.4%, and the maximum total efficiency is 18.41 ± 0.7%. Including ECC increased average yield by 0.72 L/m2 and total efficiency by 8.14% compared to standard SS. In addition, an economic study of the SS is directed, demonstrating that the MSS are 58.61% more efficient on average than the unmodified SSs.

Keywords: Absorber plate, external copper condenser, single slope solar still, productivity, rectangular channel, triangular channel, thermal analysis

1. Introduction

Freshwater is crucial for sustaining human life. Rising demand in developed and developing nations is intensifying water consumption, contributing to the expansion of arid regions worldwide (Aboulmagd *et al*., 2022; Panayotaros and Vargas-Magañathe, 2022). Water makes up around 70% of the Earth's surface; however 97% of it is salty and found in seas, while 2% is located within polar ice caps. Consequently, just 1% of the water on Earth is usable to meet basic human needs (Kim *et al*., 2022; Nezhad *et al*., 2022; Vitovsky, 2022). As the demand for clean water rises steadily over time, the available supply diminishes, leading to an escalating global water crisis (Sunil Raj and Eswaramoorthy, 2023). Around 3.5 million individuals annually die from waterborne diseases, underscoring the critical necessity for enhanced global water quality and sanitation (Jha *et al*., 2022; Mallick *et al*., 2016).

In response to this critical challenge, accelerating the distribution of clean water has become a key priority in

technological advancements and innovation (Moghadasi *et al*., 2022). Numerous techniques, including membrane desalination, multiple-effect distillation, multi-stage flash distillation, and reverse osmosis, are available for producing freshwater on a wide scale. Nevertheless, these procedures rely heavily on fossil fuels, necessitating powerful pumps and motors to raise water pressure. This dependence poses sustainability challenges, as renewable energy sources currently struggle to provide the consistent and substantial power required. An analysis is necessary to evaluate each method's mechanisms, efficiency, scalability, and feasibility, considering energy consumption, operational costs, and environmental impact. Membrane and thermal desalination techniques are effective; however, their significant energy requirements pose concerns regarding carbon emissions and long-term sustainability. Exploring advancements in renewable-powered desalination, energy recovery systems, and hybrid approaches is crucial to developing sustainable water production solutions that balance water security with environmental and economic viability (Eleiwi *et al*., 2022; M. Nazari *et al*., 2022).

Desalination methods increase greenhouse gas emissions due to their significant dependence on fossil fuels and produce effluent that contains nitrogen and phosphorus, which pollutes the environment. A sustainable way to lessen these effects is to use renewable energy sources, such as solar distillation, which minimizes the ecological footprint of freshwater production and lowers carbon emissions. The shift to renewable energy sources, especially solar distillation, provides a viable approach to address the environmental issues linked to traditional desalination methods. In contrast to fossil fuel-based methods that lead to greenhouse gas emissions and ecological harm, solar distillation utilizes plentiful and renewable solar energy, positioning it as a sustainable and low-carbon option. Compared to more energy-intensive techniques like reverse osmosis and multi-stage flash distillation, this approach uses less energy. It requires fewer mechanical components since it uses a natural evaporation-condensation cycle.

Furthermore, solar distillation significantly reduces chemical waste and brine outflow, resolving environmental issues associated with traditional desalination methods. Although other renewable-powered desalination methods, including wind and geothermal systems, have been investigated, solar distillation stands out for its ease of use, affordability, and versatility, particularly in remote and desert areas with abundant sun radiation. A comprehensive evaluation is required to assess its efficiency, scalability, and long-term viability relative to alternative desalination methods to determine its role in sustainable freshwater production (Abuşka and Kayapunar, 2021; Rezaei *et al*., 2022; Shbailat and Nima, 2021). Solar distillation is an economical and straightforward technique for generating potable water utilizing renewable energy sources (Sunil Raj and Eswaramoorthy, 2021). Solar stills primarily employ sun energy to evaporate and condense salt or brackish water into drinkable water (Alawee *et al*., 2022; Negi *et al*., 2021; Sudhakar and Cheralathan, 2021).

Solar energy represents a prevalent form of renewable energy, demonstrating greater cost-effectiveness and reduced environmental impact compared to conventional energy sources used for water purification (Rajasekaran & Murugavel Kulandaivelu, 2022). However, traditional stills have difficulty consistently maintaining a steady supply of fresh water because of fluctuations in solar intensity and heat loss through the body of SS (Mevada *et al*., 2021; Mohaisen *et al*., 2021). To increase the efficiency of sun desalination, researchers from all over the world have conducted in-depth investigations and made various adjustments to conventional solar stills. Water yield, thermal efficiency, and overall performance have been improved by innovations such as solar stills with nanostructured phase change materials (nano-PCM), modified single-slope solar stills, pyramid-shaped solar stills, slanted wick-type designs, inclined solar stills, and fin-assisted configurations. The advancements seek to optimize solar energy absorption, improve heat retention, and increase evaporation-condensation rates, thereby rendering solar desalination a more feasible and sustainable method for freshwater production (Al-Dabbas *et al*., 2021; Hassan, Yousef, Ahmed *et al*., 2020; Hassan, Yousef, Fathy, *et al*., 2020; Hassan & Yousef, 2021; R. A. Kumar *et al*., 2020). The single-slope solar still is the most recognized and thoroughly examined design within solar still systems. Research indicates that double slope solar stills (DSSSs) outperform single slope solar stills in freshwater production due to their enhanced capability to utilize solar radiation throughout the day rather than being limited to morning or afternoon hours (Hassan, Ahmed *et al*., 2020).

A 30mm graphite (Gr) absorbing plate and a cooling glass (Abd Elbar & Hassan, 2020) conducted tests showing a daily efficiency of 97.2% to 98.1 % for the modified pyramid-shaped SS compared to a regular pyramid-shaped SS. Under standard weather conditions, an SS was built with various absorber plate designs (Eltawil & Omara, 2014). The trial results indicated that combining SS with a fin-shaped absorber plate led to a 74.5% increase in productivity, alongside experiments involving an absorber plate coated with nanoparticles. The cuprous oxide nanoparticles were integrated into a jet-black paint (Al-Hamadani & Shukla, 2013). Using nanoparticles, distillate yield was increased by 16-25% over regular SS. Various energy-absorbing materials were positioned within SSs of identical dimensions for six months. The primary goal of the research was to evaluate how various energy-absorbing materials affected the production of SS distillate (Hameed, 2022; Khatod *et al*., 2022). Distillate production in an SS exhibited enhancements during the day and night following the incorporation of energy-absorbing material. Black rocks' energy absorption capacity is 20% more efficient than other rock types (Bansal *et al*., 2022).

(A. Kumar & Maurya, 2022) Al_2O_3 nanoparticles in various configurations were evaluated in wick-type solar stills,

which are utilized as basin liners in warm and cold climates. According to research, adding fins with a cotton wick significantly increases the effectiveness of solar stills, producing freshwater at rates of 4.23 kg/m² per day in the winter and 7.52 kg/m² per day in the summer. The performance of a solar still with absorber plates made of aluminum and galvanized iron was contrasted with that of a conventional solar still under the same weather circumstances (Alwan *et al*., 2021). The maximum output was achieved by combining SS and aluminium plates. (Nabil & Khairat Dawood, 2021) A modified pyramid solar absorber plate was still designed using carbon particle/nanomaterial-reinforced epoxy composites to enhance thermal efficiency. Increasing the carbon nanotube concentration in the carbon particle/epoxy composite from 2.5% to 5% resulted in 65% and 109% productivity gains, respectively. The notable enhancement is due to improved thermal conductivity, increased solar energy absorption, and more effective heat transfer, underscoring the potential of nanomaterial modifications for optimizing solar desalination efficiency (Chávez *et al*., 2021) Investigated the effectiveness of a single-slope solar still that used steel yarn fibers and hollow pin fins as absorbents. The results showed that steel wool fibers enhanced feed water flow by 25% and hollow cylindrical pin fins by 16% when compared to a standard solar still (Arunkumar, Wang, *et al*., 2020).

Reducing the glass temperature or installing a condenser (internal or exterior) are two standard methods to facilitate vapor condensation. (Arunkumar, Murugesan, *et al*., 2020) Suggest a novel design with a condenser and booster located outside the unit. The system demonstrated efficiency of approximately 79% when employing hot salt water in the home and 84% when warm water was supplied to the still until sleep. Theoretical and practical evaluations of the effect of condensation area confirm that the novel corrugated pyramid solar still (NCPSS) may achieve a maximum daily output of 4.84 kg/m² in summer and 2.69 kg/m² in winter. Using heating/cooling and nanofluid to modify the same solar still, a series of studies revealed that the external condenser contributed to a 26.3% increase in overall production. Around 10% more freshwater was produced by a modified single-slope solar still (SS) with an external condenser than by a standard SS. The improvement was seen in a single-slope solar still that included wick material, fins, and phase change materials (PCM), increasing evaporation-condensation rates and thermal efficiency (Kabeel *et al*., 2020).

The reviewed literature highlights various modifications to solar distillation units, incorporating different ancillary components to assess their impact on performance. While some researchers have explored the integration of internal condensers and additional equipment, others have investigated the benefits of combining diverse absorber plate configurations with external condensers. This study utilizes a similar condenser type; however, it is more extensive and constructed using a distinct fabrication technique. Incorporating absorber plates with varying channel shapes and sizes and an external copper condenser has enhanced freshwater yield in single-slope solar stills. Furthermore, it presents the cost analysis of the improved solar still, offering a comprehensive evaluation of the system's economic feasibility. Additionally, short-term and long-term efficiencies fluctuate over time and are independently assessed under different operating conditions, providing a detailed performance analysis of the modified solar distillation system.

2. Methods and materials

2.1. Experiment of solar still

Distillate output was evaluated using experimental setups created and built to test various absorber plate configurations and ECC. **Figure 1** shows an image of one modified experimental setup pair.

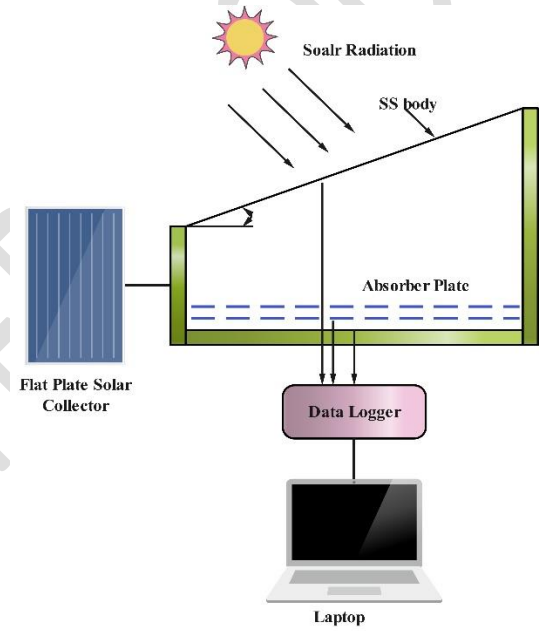

Figure 1. An Outline of modified Solar Still

The GP sheet used to make the SSs' bodies and absorber plates is 100cm thick. The CSS and MSS are similar in size of 1m^2. At the same time, the front and center sections of the side walls were 0.3m and 0.6 m in height. Water may be evaporated on its two absorber plates at the base. Cork-sheet insulation measuring 0.5m thick was used to line the stainless steel body side walls and bottom interior surfaces. The outer layer was constructed from 0.95-emissivity transparent glasses measuring 5 mm thick. The geographical orientation established a 25° angle among the horizontal plane, the solar distillate body, and the condenser surface area. The horizontal surfaces of the solar still were shielded by two panes.

Water was introduced onto a singular flat absorber plate located at the base of the CSS. In the MSS, multiple absorber plates (TC or RC) were utilized for each evaporation chamber. Absorber plates are made of GP sheets supported by hard wooden frames and feature TC and RC in various configurations. The absorber plates' free surface area for water evaporation was increased due to the introduction of channels of varying shapes. There

were 70 and 40 channels in the triangular and rectangular channel absorber plates, respectively, and both were the same size. At the experiment's outset, feed water was delivered to the SSRC and SSRCE absorbing plates until the water level reached 0.2m. Enough water was added each hour to replace what had evaporated from the absorber plates, keeping the water level constant at 0.1m. The water's exposed surface measured 0.5 m². Both absorber plates were covered in black paint to improve their ability to absorb thermal energy from solar radiation.

The CSS had an ECC attached to its top (**Figure 1**). The ECC is constructed from an 8 x 10^3 m copper tube twisted into a compression coil shape to create a hollow cylinder with a diameter of 0.5 m. Copper welding was used to narrow the spaces between the copper tubes. Polyurethane foam and tape are used to insulate the ECC's exterior, preventing heat loss to the environment. A cork-sheet base provides additional insulation. Continuous feed water from the reservoir is used to cool the ECC. Before entering the modified solar still, the feed water is directed through the hollow copper tube of the ECC to be heated by the solar collector.

2.2. Experimental procedure

The CSS, SSTCE, and SSRCE configurations were tested simultaneously and in the exact location. The experiment arrangement is depicted in **Figure 2**. a copper pipe first brought water from the reservoir to the solar still. The steady feed water flow reserved the condenser at roughly 36-39 °C, much below the inner glass's surface temperature. This method accelerated the condensation process. The latent heat that was released during condensation heated the water. The water was heated using a flat plate solar collector (FPSC) before entering the SS. Two phases of preheating the water supply led to a higher distillate output %. After condensing on the glass cover, the water vapors moved into the ECC. Both the improved SS unit and the ECC produced condensate.

The experimental equipment was placed adjacent to a pyranometer, which measures the hourly surface sun intensity. Water used in the experiment, comprising condensate collecting water and water heated by the flat plate solar collector (temperature range: 0 to 100°C), was monitored for ambient temperature using a mercury glass thermometer. A bespoke data logger tracks the temperatures of the glass, condensed air, basin water, and absorbing plates. The results are shown in **Figure 2**.

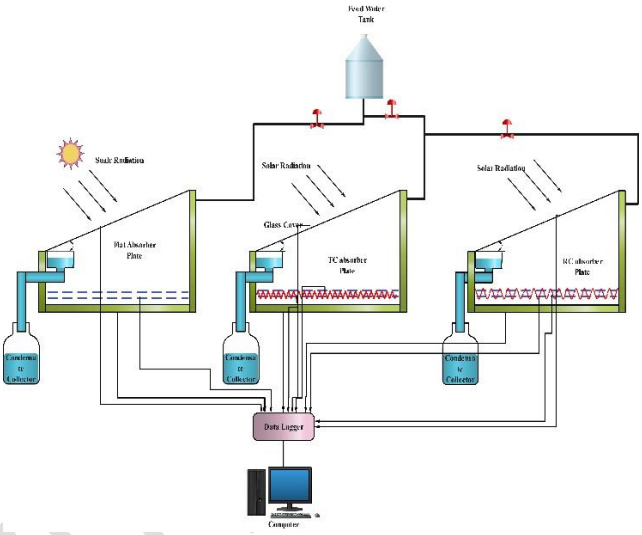

Figure 2. A modified solar still with three variant pairs of the solar distillation unit

The outer glass and the inner condenser wall temperatures were measured with an infrared thermometer. The amount of condensate produced throughout the testing was determined hourly using a levelled beaker. During each day of the trial, particular data was recorded hourly from 10:00 am to 4:00 pm. All experiments were done at the Karpagam Academy of Higher Education, Coimbatore, India (latitude 11.0168° N, 76.9558° E).

Table 1. Measurement equipment utilized in the experiment, including their ranges, accuracy, and error percentage

Equipment	Units	Accurateness	Standard uncertainty	Limits	Percentage Error
Beaker Measurement	ml	±1	0.579	0–200	±0.1
Thermocouple	◦C	±0.5	0.289	− 55 to +130	±0.5
Thermometer	◦C	±1	0.579	0–100	±0.5
Pyranometer	W/m²	±0.9	0.52	0–1290	±1
Infrared thermometer	◦ C	±0.03	0.012	0− 5 to 230	±1

2.3. Error analysis

The solar still performance is evaluated using a variety of factors. Uncertainty in the measurement process may introduce inaccuracy in a given parameter's reported values. The outcomes may be affected by these inaccuracies or percentages of uncertainty. Air temperature, external condenser temperature, absorber plate temperature, basin water temperature, outer surface temperature, inner surface temperature, ECC surface temperature, sun radiation, distillate output volume, and absorber plate temperature were all measured. Equation (1) was applied to determine the standard uncertainty of the several used devices. **Table 1** presents the instruments' measuring ranges, precisions, standard uncertainties, and error rates.

$$u = \frac{a}{\sqrt{3}} \quad (1)$$

Where u and a represent the instrument's uncertainty and accuracy, respectively.

2.4. Analysis of the rate of solar distillation unit

The cost of a solar freshwater system may be examined using the manner that has been given. The whole cost of a solar still, including the capital recovery factor (CRF), is determined using a formula,

$$CRF = \frac{i(1+i)^n}{(1+i)^n - 1} \quad (2)$$

Where i is the assumed rate of interest each year (12%) and n is the maximum useful lifespan of the SS (10 years) (S. Nazari *et al*., 2019).

$$FAC = CRF \times P \quad (3)$$

Where

FAC First Annual Cost,

P capital cost of the SS.

To determine the solar still initial annual salvage value (ASV), evaluate by,

$$ASV = SFF \times S \quad (4)$$

SS salvage value (SV) is calculated as, where C is the cost of functional equipment.

$$S = 0.2 \times P \quad (5)$$

Where

$$SFF = \frac{i}{(1+i)^n - 1} \quad (6)$$

Assuming a 15% annual maintenance cost (AMC) for stainless steel (FAC).

$$AMC = 0.15 \times FAC \quad (7)$$

Total annual SS (AC) costs are determined by

$$AC = FAC + AMC - ASV \quad (8)$$

Taking M as the typical yearly distillation yield of the solar still, it can be calculated as Cost Per Liter (CPL)

$$PL = \frac{AC}{M} \quad (9)$$

2.5. Efficacy of solar still

Instantaneous efficacy is defined as the ratio of input to output energy, providing a crucial metric for performance evaluation. In each scenario, the real-time efficiency of the solar still is analyzed. By applying numerical values to the governing formula across various conditions and time intervals, precise assessments of instantaneous efficiency can be achieved. Maximizing effectiveness involves increasing output by enhancing energy conversion efficiency and minimizing heat loss. An external condenser was also employed to boost production. Therefore, the entire instantaneous efficacy of the solar system should also be evaluated using the total convective heat exchange coefficient. Since the material is the only difference in the heat transmission between ECC and a glass surface, the two are interchangeable. For ECC, must modify Eq. (10) as,

$$n_i = \frac{q_{c,w-c}}{\alpha_w I_T} \quad (10)$$

Where, I_T rate of incident solar energy on the solar still in watts per square metre

α_w the absorption coefficient of water in (W/m^2)

So,

$$n_i = \frac{q_{c,w-g} + q_{c,w-c}}{\alpha_w I_T} \quad (11)$$

Where,

$q_{c,\,w-g} = h_{c.\,w}$, $(T_w - T_g)$ and $q_{c,\,wcc} = h_{c,\,w-c}(T_w - T_c)$

Yield per m^2 was used to determine total efficiency.

$$E = \frac{Q \times 2.4}{A \times G} \quad (12)$$

Where,

G = (W/m^2 × 60 × 60 × Hours of yield) MJ/m^2, Q = L/m^2

$$FAC = CRF \times P$$

The hourly cumulated distilled water was calculated by,

$$\sum_{h=\text{ total hour}} m_h$$

Where, m_h is the hourly yield of feed water.

3. Result and discussions

3.1. Temperatures

3.1.1. impact of solar intensity

Understanding the solar irradiation profile is crucial for determining the production capacity of distilled water by solar still. The findings demonstrated that solar irradiation rose until 13:00 h, decreasing as the sun descended. Throughout this interval, the power density of solar radiation increased from 590 W/m² to a maximum of 1050 W/m².

The rate of evaporation changed in response to the solar rays, which played a key role in the solar still ability to generate energy. On testing days, the solar rays were strongest between 13.00 and 14.00, with an 860-1060 W/m2 intensity. **Figure 3** (a) to (c) differences in water temperature between CSS, SSTCE, and SSRCE are observed. Absorber plate basin and water temperatures rise when solar irradiance increases. Basin temperatures were from 49 °C to 59 °C, 52 °C to 68 °C, and 51 °C to 65 °C for traditional solar still, TC-equipped solar still, and RC absorber plates, respectively. Water temperatures in the basins varied from 46 °C to 56 °C for traditional solar stills, 50 °C to 66 °C for solar stills with thermal collectors, and 47 °C to 61 °C for solar stills with reflective covers. At approximately 1:00 pm, when solar radiation peaks, a maximum average basin temperature of 68 °C and a maximum basin water temperature of 66 °C were recorded for SSTC. The average hourly temperatures ranged between 35 °C and 38 °C under nearly identical solar radiation conditions across all experimental days. Similarly, the average outer glass temperatures varied from 42 °C to 49 °C in each iteration, mirroring the solar radiation pattern.

3.1.2. impact of variant designing of absorbing plates

The CSS, SSTC, and SSRC absorbing plates exhibited hourly average basin water temperature variations of 46 °C to 56

°C, 51 °C to 66 °C, and 47 °C to 61 °C, respectively, under identical solar radiation profiles. The average water temperature in the basin was 4 °C to 5 °C higher for the TC absorber plate compared to the SSRC absorbing plate and the CSS. The triangular channel absorbing plate exhibited a larger surface area than the other two plate types, facilitating an enhanced heat transmission rate between the basin and the basin water. At the same time of day and under identical solar radiation conditions, **Figure 3** (a) and (b) indicate that the temperature difference between the basins was reduced in the SS with the TC absorber plate.

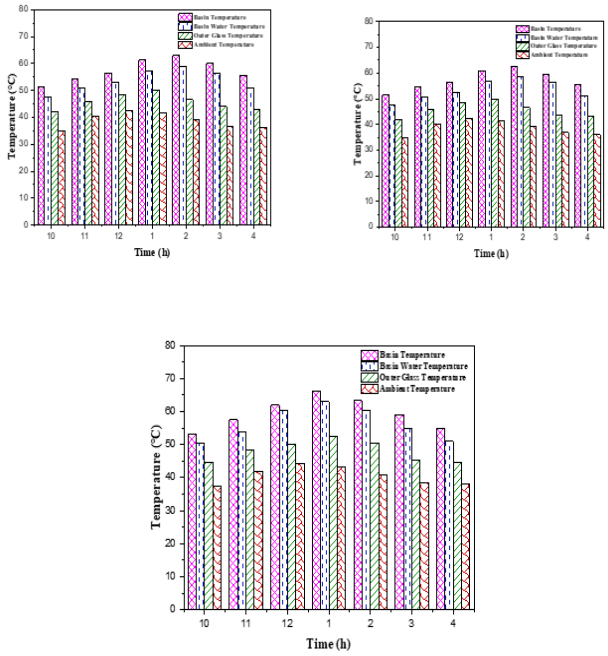

Figure 3. Variation of different factors of temperature on testing hours for (a) CSS, (b) SSTCE, and (c) SSRCE

At 1:00 pm, there was a 2 °C temperature differential between the TC absorber plate's temperature of 67 °C and the basin's average water temperature of 65 °C. In a basin with an average temperature of 65 °C, the RC absorber plate was used; the water temperature was 63 °C, creating a 4 °C temperature disparity. In CSS, the water in the basin and the mean temperature fluctuation inside the basin were both 8 °C. Temperatures varied as a consequence of the change in the absorber plate's surface area. Compared to a flat plate, absorber plates with triangular and rectangular channels have a larger surface area. An absorber plate typically has an area of 0.6 m². Instead of 0.87 m², the triangular channel absorber plate has 1.096 m² of surface area. The TC absorber plates' large surface area made the ideal heat transmission to the basin water possible. The water in the basin and around it had the least temperature difference.

Eq. (12) states that a condenser's instantaneous efficiency rises with the temperature differential between the inner surface of the glass and the basin water. As anticipated, the average instantaneous efficiency varied according to the (Tw-Tg). Higher (Tw-Tg) values were associated with improved immediate efficiency everywhere.

Instantaneous efficiency was 12.2% to 19.3 % for SSTCE, the maximum of all studied modifications, for (Tw-Tg) values between 5°C and 13°C. As a result of the warmer water in the basin, the TC and ECC enabled the SS to operate with better immediate efficiency than any of the other changes tried. The TC absorber plate's greater surface area is responsible for the enhanced heat transfer rate. As a result, the (Tw-Tg) value was maintained at a higher level than would have been the case with earlier modifications that immediately improved efficiency. SSRC and CSS plates' instantaneous efficiency was also greater than SSTCE and SSTC's, especially at lower temperature differences. When the range of (water temperature (Tw)-glass temperature (Tg)) was increased to more than 8 °C, the instantaneous efficiency of both SSTCE and SSTC increased. This was because the value of (Tw-Tg) when combining SSRC and conventional during peak solar radiation ranged from 5 °C to 8 °C (about 13.00 h).

In the morning and evening, when solar energy is lower than in the afternoon, SSTCE and SSTC showed temperature variations of 5 °C to 8 °C. The noon sun exposure hours had the most excellent evaporation rates for all the various changes. The efficiency of solar still with RC and standard absorber plates was greater than that of SS with TC during peak hours when a temperature differential of 5 °C to 8 °C was measured. When comparing solar still with and without ECC, the study found a temperature differential of 8 °C -13 °C at times of maximum solar exposure. The most considerable temperature variations across all changes were seen during high solar energy. The efficiency of TC (both with and without ECC) appeared to be increased with temperature differences. In contrast, the efficiency of SSRC and CSS systems was highest for comparatively small temperature changes.

3.1.3. impact of external copper condenser (ECC)

From 13.00 h, when the solar rays were at their strongest, the temperature of the inner glass surface rose steadily. It rises from 42 °C to 51 °C for regular SS, 45 °C to 54 °C for SS with TC, and 44 °C to 52 °C for SSRC absorber plates. When utilizing an SSTC, SSRC or flat plate absorber plate, the inner glass surface temperature might reach no more than 54 °C, 52 °C, or 51 °C, on average. Yet, ECCs typically ran between 32 °C and 40 °C (or between 33 °C and 39 °C). The ECCs created a surface temperature for condensation about 22 % lower than the inner surface. The External copper condenser kept its outer surface at a more manageable temperature because of the steady flow of feed water (at a temperature of 36 °C –39 °C) through the copper tubes of the coil. Since insulation protected the ECC, it could not have been subjected to direct sunlight. Therefore, the surface temperature of the ECC stayed relatively low and didn't rise excessively in response to the peak solar radiation. A cooling system was unavailable, and insulation was not an option due to the glass surface. As the amount of solar radiation rose, the surface temperature of the glass was also raised. As a result, ECC served as a more efficient condensing chamber

than the glass cover itself. 3.2. Collected distillation yield and efficacy

3.1.4. Impact of absorbing plates

The total distillation output in SSTCE, SSRCE, and flat plate is shown in **Figure 4**. The average distillate yield for SSTC, SSRC, and CSS after seven days was 1.63, 1.22, and 0.94 L/Day, respectively.

Compared with flat plate absorber plates and RC absorber plates, TC absorber plates resulted in a 60.8% increase in the cumulative distillate yield. Higher evaporation rates and improved heat transmission properties of the SSTCE allowed for the highest distillate yields. The surface area to volume ratio of the SSTCE absorber plate was 13.2% more than that of the RC absorber plate. Feed water evaporation and SS output both benefited from increased heat transfer area.

3.1.5. Impact of ECC

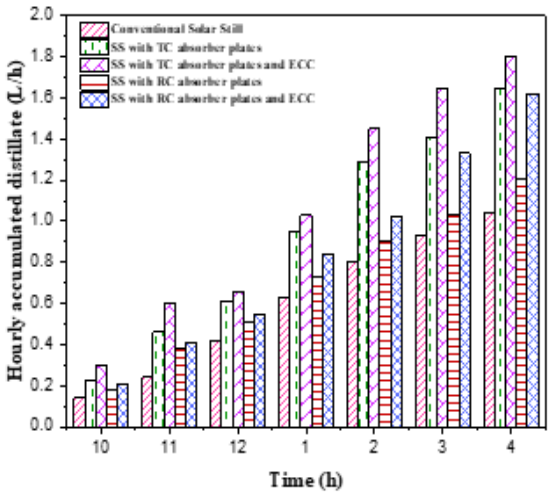

Figure 4. The sum of distillate samples taken at various times throughout the testing days for each SS variation

Figure 4 depicts the average distillate yield from employing TC and RC in modified SS with and without ECC. The mean result for triangular channel and RC absorbing plates without using ECC was 1.63 and 1.22 L/Day, correspondingly. The addition of ECC increased output to 1.74 and 1.58 L/Day. Production of SS as a whole increased due to ECC efficiency gains. Compared to TC absorber plates without an external copper condenser, those with one had a 9.8% higher overall output. On the other hand, RC absorber plates using ECC indicated a 36.12 percentage point gain. In contrast to the glass surface area intended for condensation at times of surplus vapor production at maximum solar radiation, the ECC with a glass condensing surface produced an extra 0.19 m².

3.2. Efficiency of solar stills

The average instantaneous efficiency throughout seven days of tests, with SSs occurring at different times, is shown in **Figure 5(a)**. The temperature of the inner surface of the glass has long been known to increase due to the intensity of the sun's rays, which often peak around 13.00 hours and progressively decrease during the day.

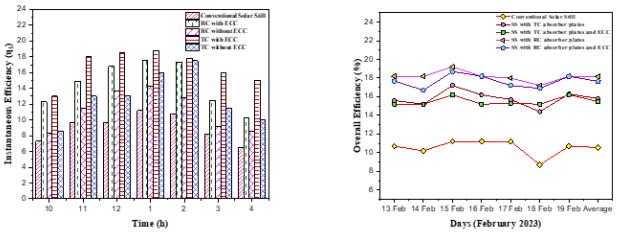

Figure 5. Evaluation of (a) instantaneous efficacy at variant hours a day, (b) total efficacy at variant testing days between variant solar stills

Eq. (11) demonstrates that the main variables affecting the instantaneous efficiency are the amount of solar radiation, the temperature of the basin water, and the condensing surface temperature. With a coiled copper coil ECC, this study tested both a triangular channel and rectangular channel absorber plate. Maximal mean instantaneous efficiencies were determined to be 15.5% ± 1.5% for TC without ECC, 13.7% ± 0.7% for RC without ECC and 10.5% ± 0.8% for conventional at 13.00 h. Due to a more significant water and glass temperature value during the topmost solar intensity, TC without ECC displayed greater immediate efficacy than the other alteration because the basin water temperature was higher without ECC.

SSTCE and SSRCE demonstrated an instantaneous efficiency increase of 2.65% and 3.2%, respectively, when equipped with ECC. The lower surface temperature provided by ECC, ranging between 32°C and 40°C, closely matched the inner glass surface temperature, contributing to the rise in immediate efficiency. This resulted in a tremendous temperature difference between the water and the glass, further enhancing efficiency. The overall efficiency comparison of the solar stills (SSs) over the seven-day experiment is presented in **Figure 5(b)**. Integration of SSTC and SSTCE in MSS yielded maximum overall efficiencies of 18.17% and 17.65 %, whereas integration of SSRC and SSRCE yielded maximum overall efficiencies of 15.8 and 15.49%. Each was collected on February 18th, 2023, the best day of the seven used in the experiment. Similarly, maximum solar radiation that day led to maximal productivity, as shown in **Figure 6**.

According to Equation (13), the total efficacy is mainly based on the total quantity of solar energy received throughout the experimental hours, the total area of the absorbing plates, and the cumulative distillate output. Therefore, the most productive day recorded was February 13-20, 2023. If one were to look at overall efficiencies on different days, it would become clear that these efficiencies varied as the solar intensity on those days transformed. Overall, the mean efficacy of the triangular and rectangular channels was raised by 2.08% and 1.96% to the ECC, respectively, compared to the experiments conducted without the ECC. Distillate accumulation rose when ECCs were utilized with TC and RC, leading to greater overall efficiency.

3.3. Yield of solar radiation

The productivity study of solar still is shown in Figure 6. The average outputs for CSS, SSTC, and SSRC absorber

plates without external copper condensers were 1.06 L/m^2, 1.41 L/m^2, and 1.35 L/m^2 in that order. The average output for SSTCE absorber plates was 1.9 L/m^2 when using ECC, whereas the average production for SSRCE was 1.56 L/m^2.

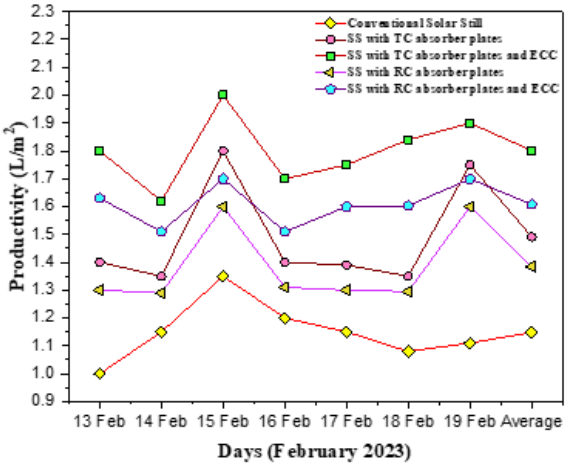

Figure 6. Evaluation of Yield of MSS and CSS of 7 testing days

By comparing redesigned solar still with and without ECC, the study found that the average output rises by 24.2% for SSTC and 20.1% for SSRC. Compared to CSS, the productivity of the variant with SSTCE grew by 64.1%, while that of the variant with SSRCE increased by 47.23 %. On 13-02-2023, TC and ECC achieved their highest production, measuring 1.9 L/m^2. Productivity is the production per unit of land per day and is the cumulative result of various changes. Since the TC absorber plate demonstrated an increased evaporation rate proportional to its surface area, more significant vapor generation was achieved, resulting in enhanced productivity. The ECC can condense more water vapor than standard SS by having a larger surface area for cooling. Therefore, the most efficient results were achieved by the integration of SSTCE.

4. Price analysis

Solar distillation technology is used primarily to lessen the carbon footprint of the final distillate product by lowering its CPL. The present work does a cost-benefit analysis of both CSS and MSS. The price-benefit study results for the different SS designs are shown in Table 2. Traditional SS has a CPL range, with a value of 1.73 ₹/L/m2 when using solely absorber plates of a different design and 1.56 ₹/L/m2 when using ECC. Among all examples, the MSS absorber plates and external copper condenser produced the highest distillate yield, making it the most cost-effective configuration. MSS necessitate an increase in the use of metal sheeting and glass. The use of expensive copper tubes in its manufacturing further raised the price. All the upgrades to the SS result in increased distillate production despite the relatively high costs associated with fabricating the upgraded absorbing plates and external copper condenser. The result was a lower cost of production per unit.

Table 2. Importance of the price analysis of MSS

Factors	SSTC/SSRC	SSTCE/SSRCE	CSS
Capital Recovery Factor	0.185	0.185	0.185
Principle cost ₹	5076	5403	4912
S	13.6	14.1	13
AC	11.77	12.528	11.391
FAC	10.85	11.55	10.5
SFF	0.057	0.057	0.057
i (amount of interest rate %)	0.13	0.13	0.13
ASV	0.71	0.752	0.684
Yearly Distillation Yield (L/m^2/ year)	621.6	694.7	402.7
AMC	1.63	1.73	1.575
n (years)	10	10	10
CPL (₹/L/ m^2)	1.56	1.47	2.29

5. Conclusion

This research involved the planning, constructing, and testing of a single slop solar still. Variations in absorber plate layout were tested, both with and without an external condenser. The solar still equipped with triangular channel absorber plates and external copper condenser, had the highest average productivity of the five variations evaluated, at 1.7 L/m^2. Compared to traditional solar still, the addition of ECC increased output by 63.4%. Average instantaneous efficiency was highest (19.3%) with SSTCE. Average instantaneous efficiency was 1.5% and 7.8% higher with SSTCE compared to SSRCE with baseline solar still respectively. Using SSTCE, the studies increased average efficiency by 19% points. The CPL for the modified SS is 1.47 /L/m^2, while the CPL for the traditional solar still is 1.56 /L/m^2. Because of this, the modified solar still had lower operating costs than the original solar still. After seven days of testing, SSTCE proved the most effective method regarding average yield and instantaneous efficacy, overall efficacy, and the average cost per liter range. As a result, SSTCE is considered the optimal upgrade.

Author's contributions

Virumandampalayam Perumal Krishnamurthy: Conceptualization, Writing and Review, **Debabrata Barik**: Review, Optimization, **Manivel Chinnappandi:** Review and

Supervision and **K. Durga Syam Prasad:** Final drafting, **Subramaniam Prabagaran:** Supervision, Review**, Kandasamy Raju**: Final drafting.

References

Abd Elbar, A. R., and Hassan, H. (2020). An experimental work on the performance of new integration of photovoltaic panel with solar still in semi-arid climate conditions. *Renewable Energy*, **146**, 1429–1443. https://doi.org/10.1016/j.renene.2019.07.069

Aboulmagd, A., Othman, H., and ElDegwy, A. (2022). Numerical Investigation of the Energetic-Exergetic Quasi-dynamic Performance of Mini-channel Solar Air Heaters. *International Journal of Renewable Energy Research*, **12**(4), 1966–1979. https://doi.org/10.20508/ijrer.v12i4.13445.g8619

Abuşka, M., and Kayapunar, A. (2021). Experimental and numerical investigation of thermal performance in solar air heater with conical surface. *Heat and Mass Transfer/Waerme- Und Stoffuebertragung*, **57**(11), 1791–1806. https://doi.org/10.1007/s00231-021-03054-5

Al-Dabbas, M., Alahmer, A., Mamkagh, A., and Gomaa, M. R. (2021). Productivity enhancement of the solar still by using water cooled finned condensing pipe. *Desalination and Water Treatment*, **213**, 35–43. https://doi.org/10.5004/dwt.2021.26711

Al-Hamadani, A. and Shukla, S. (2013). Performance of single slope solar still with solar protected condenser. *Distributed Generation and Alternative Energy Journal*, **28**(2), 6–28. https://doi.org/10.1080/21563306.2013.10677548

Alawee, W. H., Abdullah, A. S., Mohammed, S. A., Majdi, A., Omara, Z. M., and Younes, M. M. (2022). Testing a single slope solar still with copper heating coil, external condenser, and phase change material. *Journal of Energy Storage*, **56**. https://doi.org/10.1016/j.est.2022.106030

Alwan, N. T., Majeed, M. H., Shcheklein, S. E., Ali, O. M., and Praveenkumar, S. (2021). Experimental study of a tilt single slope solar still integrated with aluminum condensate plate. *Inventions*, **6**(4). https://doi.org/10.3390/INVENTIONS6040077

Arunkumar, T., Murugesan, D., Viswanathan, C., Neri, G., and Denkenberger, D. (2020). Effect of CuO, MoO3 and ZnO nanomaterial coated absorbers for clean water production. *SN Applied Sciences*, **2**(10). https://doi.org/10.1007/s42452-020-03504-5

Arunkumar, T., Wang, J., Dsilva Winfred Rufuss, D., Denkenberger, D., and Kabeel, A. E. (2020). Sensible desalting: Investigation of sensible thermal storage materials in solar stills. *Journal of Energy Storage*, **32**. https://doi.org/10.1016/j.est.2020.101824

Bansal, K., Kumar, R., Krishna Mishra, S., Kumar, P., and Sharma, A. (2022). Validation and CFD modeling of solar still with nanoparticle coating on absorber plate. *Materials Today: Proceedings*, **63**, 673–679. https://doi.org/10.1016/j.matpr.2022.04.744

Chávez, S., Terres, H., Lizardi, A., López, R., Lara, A., and Vaca, M. (2021). Numerical and Experimental Analysis in the Production of a Solar Still. *Journal of Physics: Conference Series*, **1723**(1). https://doi.org/10.1088/1742-6596/1723/1/012010

Eleiwi, M. A., Mohammed, M. F. and Kamil, K. T. (2022). EXPERIMENTAL ANALYSIS OF THERMAL PERFORMANCE OF A SOLAR AIR HEATER WITH A FLAT PLATE AND METALLIC FIBER. *Journal of Engineering Science and Technology*, **17**(3), 2049–2066.

Eltawil, M. A., and Omara, Z. M. (2014). Enhancing the solar still performance using solar photovoltaic, flat plate collector and hot air. *Desalination*, **349**, 1–9. https://doi.org/10.1016/j.desal.2014.06.021

Hameed, H. G. (2022). Experimentally evaluating the performance of single slope solar still with glass cover cooling and square cross-section hollow fins. *Case Studies in Thermal Engineering*, **40**. https://doi.org/10.1016/j.csite.2022.102547

Hassan, H., Ahmed, M. S., Fathy, M., and Yousef, M. S. (2020). Impact of salty water medium and condenser on the performance of single acting solar still incorporated with parabolic trough collector. *Desalination*, **480**. https://doi.org/10.1016/j.desal.2020.114324

Hassan, H., and Yousef, M. S. (2021). An assessment of energy, exergy and CO2 emissions of a solar desalination system under hot climate conditions. *Process Safety and Environmental Protection*, **145**, 157–171. https://doi.org/10.1016/j.psep.2020.07.043

Hassan, H., Yousef, M. S., Ahmed, M. S., and Fathy, M. (2020). Energy, exergy, environmental, and economic analysis of natural and forced cooling of solar still with porous media. *Environmental Science and Pollution Research*, **27**(30), 38221–38240. https://doi.org/10.1007/s11356-020-09995-4

Hassan, H., Yousef, M. S., Fathy, M., and Ahmed, M. S. (2020). Impact of condenser heat transfer on energy and exergy performance of active single slope solar still under hot climate conditions. *Solar Energy*, **204**, 79–89. https://doi.org/10.1016/j.solener.2020.04.026

Jha, P., Das, B., and Gupta, R. (2022). Energy matrices evaluation of a conventional and modified partially covered photovoltaic thermal collector. *Sustainable Energy Technologies and Assessments*, **54**. https://doi.org/10.1016/j.seta.2022.102610

Kabeel, A. E., El-Maghlany, W. M., Abdelgaied, M., and Abdel-Aziz, M. M. (2020). Performance enhancement of pyramid-shaped solar stills using hollow circular fins and phase change materials. *Journal of Energy Storage*, **31**. https://doi.org/10.1016/j.est.2020.101610

Khatod, K. J., Katekar, V. P., and Deshmukh, S. S. (2022). An evaluation for the optimal sensible heat storage material for maximizing solar still productivity: A state-of-the-art review. *Journal of Energy Storage*, **50**. https://doi.org/10.1016/j.est.2022.104622

Kim, J.-A., Choi, Y.-H., and Lee, W. (2022). Alteration of Inertial Focusing Positions in Triangular Channels Using Flexible PDMS Microfluidics. *Biochip Journal*, **16**(3), 342–350. https://doi.org/10.1007/s13206-022-00062-3

Kumar, A., and Maurya, A. (2022). Experimental analysis and CFD modelling for pyramidal solar still. *Materials Today: Proceedings*, **62**, 2173–2178. https://doi.org/10.1016/j.matpr.2022.03.360

Kumar, R. A., Vigneshwaran, K., and Sivakumar, V. (2020). Energy and exergy analysis of an inbuilt condenser single basin single slope solar still with zno nano particle coating. *Journal of Green Engineering*, **10**(7), 4187–4201.

Mallick, D., SHAFIQUL, I. M. D., Talukder, A., Mandol, S., Al Imran, M., and Biswas, S. (2016). *Seasonal variability in*

water chemistry and sediment characteristics of intertidal zone at Karnafully estuary, Bangladesh.

Mevada, D., Panchal, H., and Sadasivuni, K. K. (2021). Investigation on evacuated tubes coupled solar still with condenser and fins: Experimental, exergo-economic and exergo-environment analysis. *Case Studies in Thermal Engineering*, *27*. https://doi.org/10.1016/j.csite.2021.101217

Moghadasi, M., Ghadamian, H., Khodsiani, M., and Pourbafrani, M. (2022). A comprehensive experimental investigation and dynamic energy modeling of a highly efficient solar air heater with octagonal geometry. *Solar Energy*, **242**, 298–311. https://doi.org/10.1016/j.solener.2022.07.030

Mohaisen, H. S., Esfahani, J. A., and Ayani, M. B. (2021). Improvement in the performance and cost of passive solar stills using a finned-wall/built-in condenser: An experimental study. *Renewable Energy*, *168*, 170–180.

Nabil, T., and Khairat Dawood, M. M. (2021). Productivity enhancement of single-slope solar still using oxy-hydrogen gas as fuel: An experimental approach. *International Journal of Energy Research*, **45**(6), 8189–8201. https://doi.org/10.1002/er.5762

Nazari, M., Jafarmadar, S., and Khalilarya, S. (2022). Exergy and thermoeconomic analyses of serpentine tube flat-plate solar water heaters coated with CuO nanostructures. *Case Studies in Thermal Engineering*, **35**. https://doi.org/10.1016/j.csite.2022.102072

Nazari, S., Safarzadeh, H., and Bahiraei, M. (2019). Experimental and analytical investigations of productivity, energy and exergy efficiency of a single slope solar still enhanced with thermoelectric channel and nanofluid. *Renewable Energy*, **135**, 729–744. https://doi.org/10.1016/j.renene.2018.12.059

Negi, B. S., Singh, S., and Negi, S. (2021). Multiphase Numerical Modeling of PCM Integrated Solar Collector. In *Lecture Notes in Mechanical Engineering* (849–860). https://doi.org/10.1007/978-981-15-7711-6_84

Nezhad, H. M., Mohammadi, M., Ghaderi, A., Bagherzadeh, M., Ricardoc, A. M., and Kuriqic, A. (2022). Flow resistance and velocity distribution in a smooth triangular channel. *Water Supply*, **22**(5), 5253–5264. https://doi.org/10.2166/ws.2022.142

Panayotaros, P., and Vargas-Magañathe, R. M. (2022). Water wave problem with inclined walls. *European Journal of Mechanics, B/Fluids*, **96**, 108–121. https://doi.org/10.1016/j.euromechflu.2022.07.008

Rajasekaran, A. K., and Murugavel Kulandaivelu, K. (2022). Performance comparison of solar still with inbuilt condenser and agitator over conventional solar still with energy and exergy analysis. *Environmental Science and Pollution Research*, **29**(55), 83378–83388. https://doi.org/10.1007/s11356-022-21466-6

Rezaei, M., Sefid, M., Almutairi, K., Mostafaeipour, A., Ao, H. X., Hosseini Dehshiri, S. J., Hosseini Dehshiri, S. S., Chowdhury, S., and Techato, K. (2022). Investigating performance of a new design of forced convection solar dryer. *Sustainable Energy Technologies and Assessments*, **50**. https://doi.org/10.1016/j.seta.2021.101863

Shbailat, S. J., and Nima, M. A. (2021). Possible energy saving of evaporative passive cooling using a solar chimney of metal foam porous absorber. *Energy Conversion and Management: X*, **12**. https://doi.org/10.1016/j.ecmx.2021.100118

Sudhakar, P., and Cheralathan, M. (2021). Encapsulated PCM based double pass solar air heater: A comparative experimental study. *Chemical Engineering Communications*, **208**(6), 788–800. https://doi.org/10.1080/00986445.2019.1641701

Sunil Raj, B. A., and Eswaramoorthy, M. (2021). Heat Transfer Analysis on V Trough Concentrator Based Solar Air Heater with Flexible Absorber Unit. *Applied Solar Energy (English Translation of Geliotekhnika)*, **57**(1), 68–80. https://doi.org/10.3103/S0003701X21010072

SunilRaj, B. A., and Eswaramoorthy, M. (2023). Performance study on forced convection mode V-trough solar air heater with thermal storage: An experimental approach. *Materials Today: Proceedings*, **72**, 1664–1672. https://doi.org/10.1016/j.matpr.2022.09.450

Vitovsky, O. V. (2022). Experimental study of heat transfer during the flow of a gas coolant in a heated quasi-triangular channel. *International Journal of Heat and Mass Transfer*, **190**. https://doi.org/10.1016/j.ijheatmasstransfer.2022.122771